Geochemical Perspectives Letters

Accurate equilibrium Δ_{47}-Δ_{48} values in bivalves despite bulk differences in inner layer

A.N. Curley[1*], N.J. de Winter[2], B. Oerlemans[2], M. Peharda[3], J. Fiebig[1]

OPEN ACCESS

https://doi.org/10.7185/geochemlet.2632

Abstract

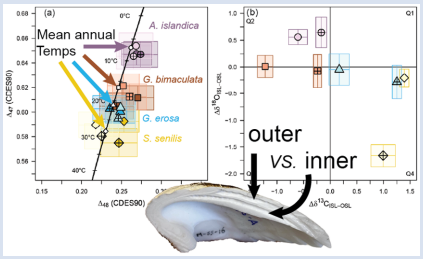

Dual clumped isotope (Δ_{47}-Δ_{48}) measurements are a relatively new palaeothermometry technique with an inbuilt "check" on the equilibrium state of carbonate minerals. Bulk shells of bivalves seem not to be kinetically biased in Δ_{47}, making them potentially ideal palaeoclimate archives. A few examples of bivalves with kinetically biased Δ_{47} localised to the inner shell layer or juvenile portion exist, but mounting evidence documents systematic $\delta^{18}O$ and $\delta^{13}C$ differences between the inner and outer shell layers. We present the first inter-layer comparisons using high precision Δ_{47}, Δ_{48}, $\delta^{18}O$, and $\delta^{13}C$ measurements of the bivalves *Arctica islandica*, *Glycymeris bimaculata*, *Senilia senilis*, and *Geloina erosa* from different climatic areas. Δ_{47}-Δ_{48} values for all these species are within local annual temperature ranges and reproduce mean annual or growing season temperatures within 0.2–3.8 °C, regardless of anatomical layer. Inter-layer differences in $\delta^{18}O$ and $\delta^{13}C$ exist, with outer layers most consistent between individuals from the same location. These results support bivalve shells being equilibrium Δ_{47}-Δ_{48} palaeotemperature archives and underscore that anatomical position of bulk $\delta^{18}O$ and $\delta^{13}C$ samples should be scrutinised even for equilibrium archives.

Received 30 January 2026 | Accepted 30 June 2026 | Published 10 September 2026

Introduction

Biogenic carbonates are important palaeoclimate archives, providing long term perspectives on climate change and contextualising major biosphere transitions throughout Earth history. The $\delta^{18}O$ composition of skeletal carbonates such as corals, foraminifera, and bivalves are often measured to reconstruct marine palaeotemperatures (*e.g.*, Chen and Watkins, 2025). However, this requires knowledge of the isotopic value of formation water ($\delta^{18}O_{water}$). Clumped isotope measurements circumvent the need for *a priori* $\delta^{18}O_{water}$ quantities by recording palaeotemperature independently, which can subsequently be used alongside carbonate $\delta^{18}O$ to calculate $\delta^{18}O_{water}$ empirically (Huntington and Petersen, 2023). In thermodynamic equilibrium, bonding between "heavy" oxygen and carbon isotopes within the carbonate lattice varies exclusively with mineralisation temperature (Ghosh *et al.*, 2006; Schauble *et al.*, 2006). Therefore, the excess abundance of multiply substituted ("clumped") isotopologues of CO_2 evolved from $CaCO_3$ compared to the predicted abundance based on randomly arranged isotopes (Δ_{47}) functions as a well calibrated palaeothermometer (*e.g.*. Kelson *et al.*, 2017; Anderson *et al.*, 2021). This has improved records of palaeohydrological dynamics underpinned by reconstructed $\delta^{18}O_{water}$ (Huntington and Petersen, 2023 and refs therein).

Carbonates that originally precipitate out of thermodynamic equilibrium (*e.g.*, corals, brachiopods, coccoliths; Davies *et al.*, 2022, 2023; Clark *et al.*, 2025) violate preconditions for Δ_{47} palaeothermometry, but can be identified less ambiguously using dual clumped isotope analysis (Δ_{47} plus Δ_{48}) (*e.g.*, Bajnai *et al.*, 2020; Davies *et al.*, 2022, 2023). Because Δ_{48} is similarly controlled by temperature but concerns different CO_2 isotopologues, a temperature dependent equilibrium between Δ_{47} and Δ_{48} exists, which has been constrained by Fiebig *et al.* (2021, 2024) considering *ab initio* thermodynamic predictions related to bond energies (Hill *et al.*, 2014) plus empirical measurements of carbonates that crystallised closest to equilibrium. Moreover, the equilibrium Δ_{47}-Δ_{48}-T relationships for calcite remain valid for other common biomineral $CaCO_3$ polymorphs, including aragonite (Bernecker *et al.*, 2025). With Δ_{47}-Δ_{48} measurements, disequilibrium signals can provide new insight into biomineralisation processes even if not primary growth temperature.

Bivalve shells are favoured palaeoclimate archives due to frequently good preservation in the fossil record and their ubiquity across aquatic environments. Schlidt *et al.* (2025) measured the Δ_{47}-Δ_{48} composition of 14 modern marine bivalve species, finding only one analytically distinguishable from Δ_{47}-Δ_{48} equilibrium. Curley *et al.* (2023), Gey *et al.* (2024), and Lollos *et al.* (2025) recently showed that some bivalves have a heterogeneous isotopic composition in different structural layers, frequently in $\delta^{18}O$ and $\delta^{13}C$ but only significantly in Δ_{47} in two fossil species. Schlidt *et al.* (2025) were unable to address mixing effects from isotopically distinct layers as they crushed and homogenised valves wholesale. Lollos *et al.* (2025) made the first attempt at measuring dual clumped isotopes in different layers of modern bivalve shells,

1. Institute for Geosciences, Goethe Universität-Frankfurt, Frankfurt am Main 60438, Germany
2. Department of Earth Sciences, Vrije Universiteit Amsterdam, Amsterdam 1081 HV, The Netherlands
3. Institute of Oceanography and Fisheries, Split 21000, Croatia
* Corresponding author (email: Curley@em.uni-frankfurt.de)

but problems with standardisation and low replication led to relatively high uncertainty in Δ_{48}. So, to date there have still been no high precision Δ_{47}-Δ_{48} measurements on the different layers of bivalve shells.

Here we present layer-specific dual clumped isotope measurements of four bivalve species. All specimens were collected live from natural environments with directly monitored water temperatures at two of four locations. Time synchronous sampling of the outer shell layer (OSL) and inner shell layer (ISL) allowed robust comparison of compositions. The Δ_{47}, Δ_{48}, $\delta^{18}O$, and $\delta^{13}C$ values were assessed for their fidelity to environmental values and discussed for their implications on future palaeoclimate applications of dual clumped isotopes in bivalves.

Methods

Samples. Four bivalve species, aragonitic in both layers, were measured for dual clumped isotopes (Fig. 1): *Arctica islandica* (North Sea, Norway), *Glycymeris bimaculata* (Pag Bay, Croatia), *Senilia senilis* (Atlantic Ocean, Mauritania), and *Geloina erosa* (brackish mangrove, Indonesia). Specimens were collected live with articulated valves. Shells longer than 3 cm were selected to ensure sufficient sample sizes.

We sampled one valve each from two different individuals of these species to assess reproducibility. Each valve was sectioned along the axis of maximum growth using a water cooled saw and cut faces were polished to a ~15 µm finish to highlight growth banding and the OSL-ISL boundary. The organic-rich periostracum and ligaments were removed before sampling. Samples of ~100 mg were milled with a hand drill at 3000 rpm, making consistent slow passes over the entire sampling area and taking frequent ~10–30 s breaks to minimise frictional heating (Fig. 2).

Clusters of at least two mid-life growth increments traceable across the OSL-ISL boundary under magnification were selected (Fig. 2a). These bands were milled out in the OSL and ISL separately, ensuring that the same part of ontogeny was represented in both samples from the same shell, but different years may have been sampled in the second shell for that species based on different sizes and band visibility. The thin shell of *G. erosa* required milling a strip the entire thickness of the ISL to yield 100 mg (Fig. 2b). This represents a lifetime average of material, so an equivalent transect from hinge to commissure of the OSL was drilled externally. It was possible to visually confirm that OSL and ISL material did not mix in cross sectional view, despite coming from different faces. Powders were manually homogenised and aliquoted in 7–9 replicates of 10.0 ± 0.2 mg. The powders remained in a vacuum oven at 30 °C for at least two weeks prior to analysis to prevent isotopic exchange with adsorbed water (Staudigel *et al.*, 2025).

Isotopic analysis. Samples were digested in 108 % phosphoric acid in a common acid bath at 90 °C as described in Fiebig *et al.* (2019). Heated (1000 °C) and equilibrated (25 °C) gas standards were run as described in Bernecker *et al.* (2023). Mass spectrometric raw data was processed using the D4xgui app (Bernecker *et al.*, 2026), including correction of raw *m/z* 47–49 intensities for the pressure baseline, data anchoring relative to nominal Δ_{47} and Δ_{48} of equilibrated gases (Fiebig *et al.*, 2021), and full error propagation considering mass spectrometric measurements and data standardisation. Δ_{47} and Δ_{48} are reported in CDES90 and 95 % confidence intervals (CI) are considered for data interpretation. When aggregating data from multiple samples, Monte Carlo simulations ($n = 10{,}000$) considering sample means and standard error resulting from the former data processing were used.

Environmental data sets. Environmental temperature data for the sampling locations were compiled from various sources.

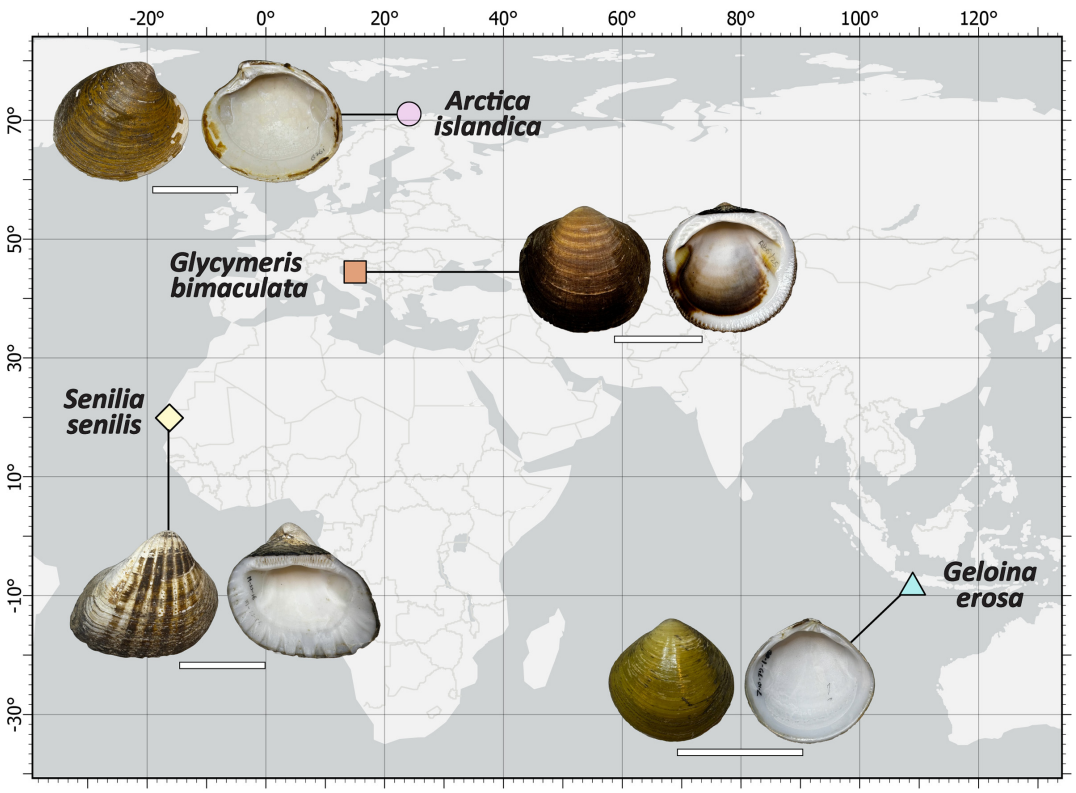

Figure 1 Sampling locations. Symbols and colours correspond to subsequent figures. Scale bars = 2 cm. Basemap: Esri World Countries Generalised 2022 (Sources: Esri, Garmin, and U.S. Central Intelligence Agency (The World Factbook)).

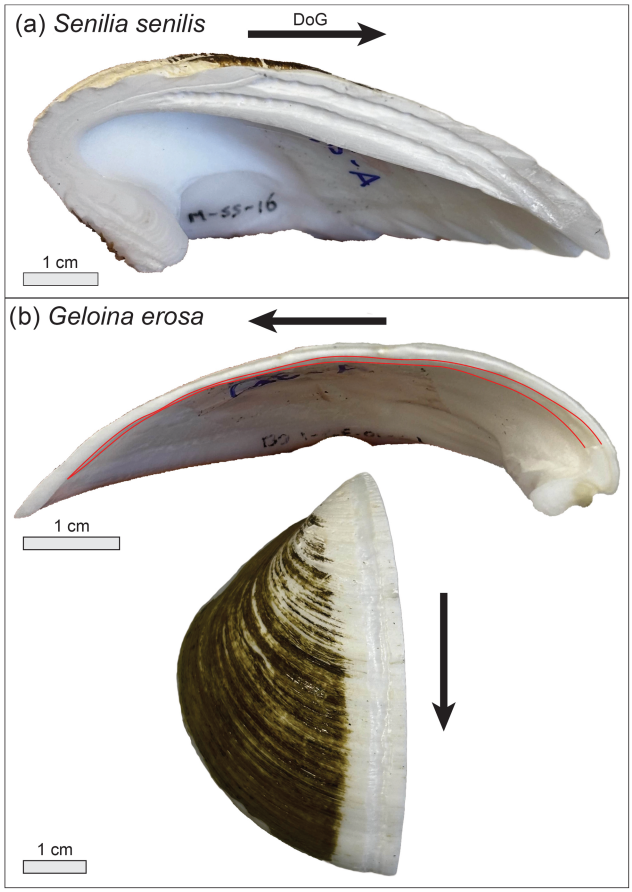

Figure 2 Example drill paths. **(a)** Cross sectional approach showing time synchronous growth bands milled. **(b)** Exterior approach showing the entire ISL thickness milled (red outline) and the entire OSL hinge-commissure transect milled (below). Black arrows show direction of growth (DoG).

In all but one case, the duration of these records includes the actual lifetime of the shells based on collection dates. For *G. bimaculata*, the *in situ* record begins the year after sample collection, and the low inter-year variability in that record indicates that extrapolation to the recent lifetime of the animal is reasonable.

For *A. islandica*, monthly mean water temperature data (direct measurements, 5 m depth) were extracted from publicly accessible data from the Ingøya monitoring station of the Norwegian Institute for Marine Research (https://www.imr.no/forskning/forskningsdata/stasjoner/view?station=Ingoy). We compiled data from 2013–2020 (samples collected in 2020) to obtain at least five observations for each month. For *G. bimaculata*, daily water temperature data (direct measurements, 3–4 m depth) from 2015–2020 (samples collected in 2014) for Pag Bay were contributed by the Institute of Oceanography and Fisheries (Split, Croatia) (*e.g.*, Vilibić *et al.*, 2022). For *S. senilis* and *G. erosa*, we used the interpolated data product from the World Ocean Atlas (WOA) 2023 at 0.25° resolution (Locarnini *et al.*, 2024). Monthly mean temperature data for 0–10 m were extracted from the nearest appropriate grid cell to the sampling location. The 2015–2022 and 2005–2014 data products were used for *S. senilis* (samples collected in 2021) and *G. erosa* (samples collected in 2010), respectively.

Results

Dual clumped isotopes. All samples but one *G. bimaculata* OSL were in equilibrium (*i.e.* the 95 % CI overlapped the equilibrium line of Fiebig *et al.*, 2024) (Fig. 3a). Within each valve, the difference between OSL and ISL temperatures was smaller than the 95 % CIs, which overlapped significantly, rendering them all analytically indistinguishable. For all samples, the mean annual water temperature (MAT) was contained within the 95 % confidence window (Fig. 3c–f), including the disequilibrium *G. bimaculata* sample, indicating that only Δ_{48} was significantly positively biased.

Temperatures derived from sample mean Δ_{47} values were within 3.8 °C of either MAT or growing season temperature (GST) in all cases (Fig. 3c–f, Table 1). The mean difference between the Δ_{47} temperature and relevant environmental mean was 1.6 ± 2.6 °C (2 s.d.). Binning four *A. islandica* samples, the mean Δ_{47} temperature was 7.1 ± 4.7 °C (2 s.e.), where MAT and GST were 6.9 °C and 7.2 °C, respectively. The total temperature range from individual samples including the 95 % CIs (3.3–10.3 °C) is almost the same size as the total annual water temperature range (3.9–10.7 °C). Binning four *G. bimaculata* samples, the mean Δ_{47} temperature was 18.9 ± 6.0 °C (2 s.e.), where MAT and GST temperature were 16.5 °C and 19.2 °C, respectively. For all individual samples, the entire 95 % CI (13.8–23.9 °C) was within the total seasonal temperature range (6.7–28.6 °C) but skewed towards the GST. Binning four *S. senilis* samples, the mean Δ_{47} temperature was 23.0 ± 5.0 °C (2 s.e.), where MAT was 21.1 °C. The total temperature range from individual samples including the 95 % CIs (19.9–27.3 °C), aligned better with warmer months within the full seasonal water temperature range (16.7–27.2 °C). Binning four *G. erosa* samples, the mean Δ_{47} temperature was 28.7 ± 7.0 °C (2 s.e.), where MAT was 28.3 °C. Although all 95 % CIs (23.7–34.8 °C) overlapped the total seasonal temperature range (25.7–29.9 °C), together their range is several degrees wider than the recorded environmental temperatures.

Bulk isotopic composition. Absolute OSL $\delta^{18}O$ values from the two individuals of each species were analytically indistinguishable in all cases (Table 1). Absolute OSL $\delta^{13}C$ values were all analytically indistinguishable except *S. senilis*, where the two differed by 0.43 ‰ (2 s.d. < 0.2 ‰) (Table 1). In contrast, ISL $\delta^{18}O$ values were all indistinguishable except for *G. erosa*, where the two differed by 1.40 ‰ (2 s.d. < 0.2 ‰), and ISL $\delta^{13}C$ values were distinguishable in every case with differences ranging from 0.28 to 0.93 ‰ (2 s.d. 0.03–0.11 ‰) (Table 1).

All but one shell (*G. bimaculata*) had measurable differences between ISL and OSL $\delta^{18}O$ and/or $\delta^{13}C$ values ($\Delta\delta^{18}O_{ISL\text{-}OSL}$, $\Delta\delta^{13}C_{ISL\text{-}OSL}$) (Fig. 3b). Altogether, $\Delta\delta^{18}O_{ISL\text{-}OSL}$ values spanned −1.66 to +0.65 ‰ and $\Delta\delta^{13}C_{ISL\text{-}OSL}$ spanned −1.22 to +1.39 ‰. Among individuals of the same species, the magnitudes of these offsets differed but their directionality was largely the same. *A. islandica* fell in quadrant 1 ($+\Delta\delta^{18}O_{ISL\text{-}OSL}$, $-\Delta\delta^{13}C_{ISL\text{-}OSL}$). *G. bimaculata* had $\Delta\delta^{18}O_{ISL\text{-}OSL} \approx 0$ ‰ and $-\Delta\delta^{13}C_{ISL\text{-}OSL}$ values, the larger of which come from the specimen biased in Δ_{48}. *S. senilis* and *G.erosa* fell in quadrant 4 ($-\Delta\delta^{18}O_{ISL\text{-}OSL}$, $+\Delta\delta^{13}C_{ISL\text{-}OSL}$ values).

Discussion

Dual clumped isotopes record MAT/GST highly accurately. It is uncertain whether the *S. senilis* Δ_{47} temperatures were truly warm season biased as it appears (Fig. 3e) because WOA data down to 10 m were averaged, potentially including waters cooler than the true shallow growth environment. A similar consideration is true for *G. erosa*, plus the real seasonality in a shallow, tidal mangrove where summer water temperatures can exceed 30 °C (Soeprobowati *et al.*, 2023) is very likely greater than the offshore data point. In both cases employing WOA data, density

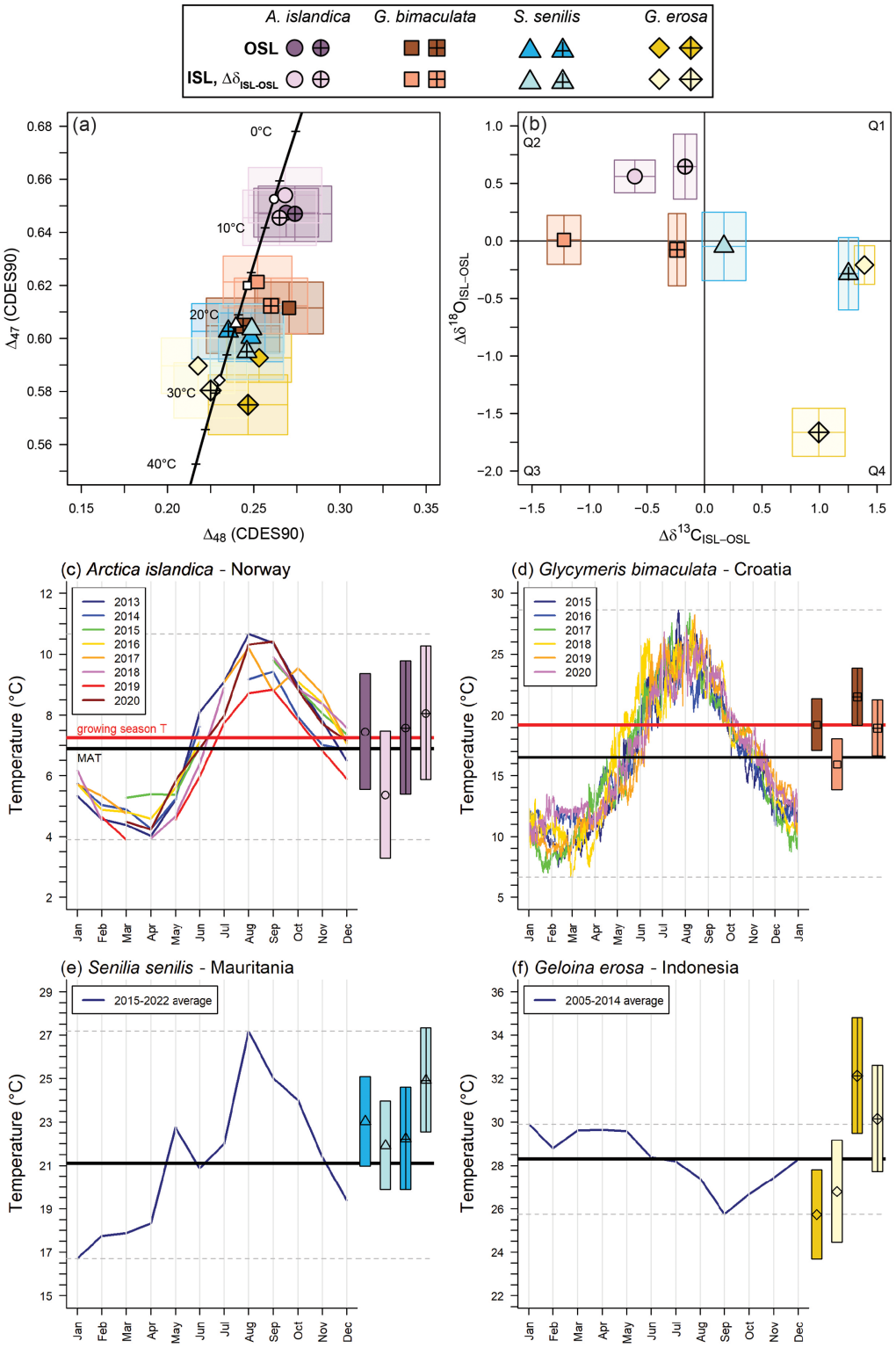

Figure 3 **(a)** Δ_{47}-Δ_{48} equilibrium line (Fiebig *et al.*, 2024). Symbols and colours correspond to species: darker values the OSL, lighter values the ISL. Internal crosses differentiate two individuals. Shaded boxes show 95 % CI. White symbols along equilibrium line show MAT for species with corresponding shape. **(b)** $\Delta\delta^{18}O_{ISL\text{-}OSL}$ *vs.* $\Delta\delta^{13}C_{ISL\text{-}OSL}$. ISL colour values used arbitrarily to visually unify the two specimens, with OSL and ISL values collapsed into single points by subtraction. Shaded boxes show propagated 2 s.e. Quadrants labelled Q1-Q4 in extreme corners. **(c–f)** Environmental temperatures. Temperature curves (left) differentiate years by colour. Δ_{47} temperatures (right) show boxes spanning 95 % CI. Grey dashed lines highlight absolute maximum and minimum environmental temperatures. Thick black lines show MAT. Thick red lines show mean growing season temperature (GST) (*A. islandica*: March–November; *G. bimaculata*: May–December).

of instrumental measurements affects the fidelity of temperatures, and the multi-year monthly averaging masks extremes in given months/years that the instrumental data resolves.

Both the OSL and ISL record comparable temperatures. The one non-equilibrium sample could be strictly fortuitous (a 5 % probability) or might indicate slightly elevated levels of

Table 1 Summary of collection locations, isotopic results for OSL and ISL, and environmental water data.

ID	Lat	Long		$\delta^{13}C$ (VPDB) Mean ± 2 s.d.	$\delta^{18}O$ (VPDB) Mean ± 2 s.d.	Δ_{47} (CDES90) Mean ± 95 % CI	Δ_{48} (CDES90) Mean ± 95 % CI	Δ_{47}-*T* (°C) min–max (mean)	Water *T* (°C)	
Arctica islandica (collected 11/1/2020)										
AI-A	71.06	24.10	OSL	2.05 ± 0.12	2.58 ± 0.07	0.65 ± 0.01	0.27 ± 0.02	5.6–9.4 (7.4)	Range	3.9–10.7
			ISL	1.44 ± 0.06	3.14 ± 0.08	0.65 ± 0.01	0.27 ± 0.02	3.3–7.5 (5.4)	MAT	6.9
AI-B	71.06	24.10	OSL	1.89 ± 0.05	2.55 ± 0.17	0.65 ± 0.01	0.27 ± 0.02	5.4–9.8 (7.6)	GST	7.2
			ISL	1.72 ± 0.05	3.20 ± 0.11	0.65 ± 0.01	0.27 ± 0.02	5.9–10.3 (8.1)		
Glycymeris bimaculata (11/1/2014)										
GB-A	44.46	15.03	OSL	1.51 ± 0.08	1.27 ± 0.12	0.61 ± 0.01	0.27 ± 0.02	17.1–21.4 (19.2)	Range	6.7–28.6
			ISL	0.29 ± 0.06	1.27 ± 0.17	0.62 ± 0.01	0.25 ± 0.02	13.8–18.0 (15.9)	MAT	16.5
GB-B	44.46	15.03	OSL	1.46 ± 0.05	1.21 ± 0.08	0.60 ± 0.01	0.24 ± 0.02	19.2–23.9 (21.5)	GST	19.2
			ISL	1.22 ± 0.03	1.14 ± 0.15	0.61 ± 0.01	0.26 ± 0.02	16.7–21.3 (18.9)		
Geloina erosa (collected 2010)										
GE-A	−7.71	108.88	OSL	−12.13 ± 0.05	−4.56 ± 0.07	0.59 ± 0.01	0.25 ± 0.02	23.7–27.8 (25.7)	Range	25.7–29.9
			ISL	−10.74 ± 0.04	−4.77 ± 0.10	0.59 ± 0.01	0.22 ± 0.02	24.5–29.2 (26.8)	MAT	28.3
GE-B	−7.71	108.88	OSL	−12.26 ± 0.15	−4.51 ± 0.11	0.58 ± 0.01	0.25 ± 0.02	29.5–34.8 (32.1)		
			ISL	−11.26 ± 0.08	−6.17 ± 0.10	0.58 ± 0.01	0.23 ± 0.02	27.7–32.6 (30.1)		
Senilia senilis (collected 9/1/2021)										
SS-A	19.90	−16.25	OSL	−0.98 ± 0.08	0.95 ± 0.17	0.60 ± 0.01	0.25 ± 0.02	21.0–25.1 (23.0)	Range	16.7–27.2
			ISL	−0.81 ± 0.11	0.90 ± 0.12	0.60 ± 0.01	0.25 ± 0.02	19.9–24.0 (21.9)	MAT	21.1
SS-B	19.90	−16.25	OSL	−1.41 ± 0.03	1.09 ± 0.20	0.60 ± 0.01	0.24 ± 0.02	19.9–24.6 (22.2)		
			ISL	−0.16 ± 0.06	0.81 ± 0.11	0.60 ± 0.01	0.25 ± 0.02	22.5–27.3 (24.9)		

organics (Fiebig *et al.*, 2024). Even with accurate equilibrium clumped isotope temperatures, different bulk $\delta^{18}O$ in the two layers would still bias $\delta^{18}O_{water}$ reconstructions. Inter-layer homogeneity should be assessed prior to using Δ_{47} and $\delta^{18}O$ to calculate $\delta^{18}O_{water}$. Good agreement between OSL values from the same location across different specimens suggests that the OSL is better for reconstructing $\delta^{18}O_{water}$ than the ISL (Table 1).

Our accurate temperature reconstructions evidence the validity of drilling as a preparation method, despite previous experiments where frictional heating induced with high drill speeds in small areas partially reset Δ_{47} temperatures (*e.g.* Staudigel and Swart, 2016; Staudigel *et al.*, 2023). Although there still may be some reordering or aragonite-to-calcite conversion (Staudigel and Swart, 2016 noted 95–100 % aragonite at drill speeds of 4000 rpm), comparisons between our hand drilled samples and environmental temperatures indicate that any effect from this preparation bias is dwarfed by analytical uncertainty and natural seasonality. Frictional heating from drilling should be a minimal concern when following cautious procedures as done here (low speed and pressure, constant motion, and short intermittent contact periods), especially when the sample material is not very resistant to milling as are most recent and well preserved fossil bivalves.

Considering the near total lack of intra-specific differences in $\delta^{18}O$ and $\delta^{13}C$ values deriving from the OSL, it appears that external dissolved inorganic carbonate (DIC) is likely compositionally identical for the two specimens collected at each location. Different OSL $\delta^{13}C$ among the two *S. senilis* shells could be due to the samples reflecting different growth years wherein bottom water $\delta^{13}C$ varied, but indistinguishable $\delta^{18}O$ and temperatures limit confidence in upwelling or freshening as potential causes. Alternatively, variable DIC of porewaters surrounding the burrowing shells could be important and tend to vary in $\delta^{13}C$ more than $\delta^{18}O$ due to microbial activity.

The intra-specific variation in $\Delta\delta^{13}C_{ISL\text{-}OSL}$ and $\Delta\delta^{18}O_{ISL\text{-}OSL}$ could be driven by either kinetic or source effects. Considering all samples, there is no strong correlation between $\Delta\delta^{18}O_{ISL\text{-}OSL}$ and $\Delta\delta^{13}C_{ISL\text{-}OSL}$, not supporting prevalent kinetic control on the bulk isotopic composition. Some evidence suggests that $\delta^{18}O$ may be more susceptible to kinetic effects than Δ_{47} or Δ_{48} due a combination of higher measurement precision and slower equilibration at the $CaCO_3$-H_2O interface depending on mineral surface characteristics (Schlidt *et al.*, 2025), but even if minor kinetic effects exist here, source effects likely overshadow them.

The immediate DIC source for the ISL might become measurably distinct from ambient water firstly by isotopic modification of internal DIC by numerous metabolic processes (*e.g.*, respiration, tissue maintenance, digestion, reproduction), and secondly when that modified internal DIC is transformed into extrapallial (calcifying) fluid. If the same or different fractionating processes occur when secreting the outer extrapallial fluid (which may or may not be the case), mixing with ambient water may overprint this physiologically derived signal, leading to very consistent OSL $\delta^{18}O$ and $\delta^{13}C$ values, whereas the ISL values preserve it.

Members of the same species occupying the same quadrant in Figure 3 demonstrate an inherent consistency in the pathways fractionating internal DIC on the species level due to

shared physiology, but the differences in absolute magnitudes of $\Delta\delta^{18}O_{ISL\text{-}OSL}$ and $\Delta\delta^{13}C_{ISL\text{-}OSL}$ values could be due to individual level factors like metabolic rate, diet, reproduction, and valve closure variably influencing internal DIC (*e.g.*, Curley *et al.*, 2023 and refs. therein). Additionally, the spread of values further affirms that these fundamental fractionating pathways can vary among different species of bivalves, as previously reported (*e.g.*, Lollos *et al.*, 2025; Curley *et al.*, 2023).

Some of *G. erosa*'s large $\Delta\delta^{18}O_{ISL\text{-}OSL}$ and $\Delta\delta^{13}C_{ISL\text{-}OSL}$ values could be due to their unique ecology as a tidal species (Purba *et al.*, 2025), where in different years they may have experienced more meaningfully different behaviours, freshwater inputs, and DIC sources. They also have $\delta^{13}C$ values in either layer consistently at least 10 ‰ lower than any of the other species (Table 1), possibly consistent with relatively high incorporation of metabolic DIC in the calcifying fluid carbon budget due to more time spent with valves closed during low tide (*e.g.*, Gillikin *et al.*, 2007).

Conclusions

Δ_{47} temperatures from hand drilled *A. islandica*, *G. bimaculata*, *S. senilis*, and *G. erosa* shells were consistently within 3.8 °C (on average 1.6 °C) of environmental mean temperatures. Δ_{47}-Δ_{48} values fell on the equilibrium line in all except one case, wherein the Δ_{47} temperature remained accurate. Temperatures reconstructed from either OSL or ISL carbonate in the same shell were analytically indistinguishable, but $\delta^{18}O$ and $\delta^{13}C$ varied systematically. Inter-layer $\delta^{18}O$ and $\delta^{13}C$ offsets indicate some amount of physiological influence, likely driven by source effects. The directionality of these is consistent among individuals of the same species, suggesting a common mechanism. In some cases, $\Delta\delta^{18}O_{ISL\text{-}OSL}$ values are great enough to meaningfully bias reconstructed $\delta^{18}O_{water}$ if the ISL is sampled, despite accurate Δ_{47} temperatures, highlighting the importance of considering intra-shell variability when using bivalve shells as hydroclimate archives.

Acknowledgements

We would like to acknowledge assistance from Jan van Gils (*S. senilis*), Rob Witbaard (*A. islandica*) and Simon Troelstra (*G. erosa*) in acquiring some of the specimens used in this work. We thank Miguel Bernecker, Sven Hofman, Niels Meijer, and Philip Staudigel for assistance in the lab. JF was supported through DFG, Reinhart Koselleck project FI-948/13–1, NJW and BO were financially supported by the Netherlands Research Council (NWO) through a personal VENI fellowship awarded to NJW (*MACRO*, VI.Veni.222.354). NJW was supported by funds from the "Sectorplan Beta and Techniek" by the Dutch Ministry for Education, Culture and Science. MP was supported by CSF project BivalveSPEECH (IP-2024-05-2190). This manuscript was improved by the contribution of editorial and anonymous peer review.

Editor: Eric Oelkers

Additional Information

Supplementary Information accompanies this letter at https://www.geochemicalperspectivesletters.org/article2632.

Cite this letter as: Curley, A.N., de Winter, N.J., Oerlemans, B., Peharda, M., Fiebig, J. (2026) Accurate equilibrium Δ_{47}-Δ_{48} values in bivalves despite bulk differences in inner layer. *Geochem. Persp. Let.* 41, 46–52. https://doi.org/10.7185/geochemlet.2632

References

Anderson, N.T., Kelson, J.R., Kele, S., Daëron, M., Bonifacie, M., Horita, J., Mackey, T.J., John, C.M., Kluge, T., Petschnig, P., Jost, A.B., Huntington, K.W., Bernasconi, S.M., Bergmann, K.D. (2021) A Unified Clumped Isotope Thermometer Calibration (0.5–1,100°C) Using Carbonate-Based Standardization. *Geophysical Research Letters* 48, e2020GL092069. https://doi.org/10.1029/2020GL092069

Bajnai, D., Guo, W., Spötl, C., Coplen, T.B., Methner, K., Löffler, N., Krsnik, E., Gischler, E., Hansen, M., Henkel, D., Price, G.D., Raddatz, J., Scholz, D., Fiebig, J. (2020) Dual clumped isotope thermometry resolves kinetic biases in carbonate formation temperatures. *Nature Communications* 11, 4005. https://doi.org/10.1038/s41467-020-17501-0

Bernecker, M., Hofmann, S., Staudigel, P.T., Davies, A.J., Tagliavento, M., Meijer, N., Ballian, A., Fiebig, J. (2023) A robust methodology for triple (Δ_{47}, Δ_{48}, Δ_{49}) clumped isotope analysis of carbonates. *Chemical Geology* 642, 121803. https://doi.org/10.1016/j.chemgeo.2023.121803

Bernecker, M., Bonifacie, M., Staudigel, P., Meijer, N., Siebert, J., Wehr, N., Haussühl, E., Bernasconi, S.M., Petrash, D.A., Dietzel, M., Fiebig, J. (2025) Effects of mineralogy on Δ_{47} and Δ_{48} of carbonate-derived CO_2 below analytical resolution. *Geochimica et Cosmochimica Acta* 401, 89–103. https://doi.org/10.1016/j.gca.2025.06.004

Bernecker, M., Daëron, M., Staudigel, P.T., Hofmann, S., Fiebig, J. (2026) D4Xgui: A tool for baseline correction and standardization of carbonate clumped isotope raw data. *SoftwareX* 33, 102492. https://doi.org/10.1016/j.softx.2025.102492

Chen, S., Watkins, J.M. (2025) Oxygen and Carbon Isotopes in Marine Carbonates: A Biogenic Climate Archive Built Upon Disequilibria. *Elements* 21, 112–117. https://doi.org/10.2138/gselements.21.2.112

Clark, A.J., Jaggi, M., Bernasconi, S.M., Fiebig, J., Stoll, H.M. (2025) Clumped Isotope Temperatures of Coccolithophores From Global Sediment Traps. *Paleoceanography and Paleoclimatology* 40, e2024PA005054. https://doi.org/10.1029/2024PA005054

Curley, A.N., Petersen, S.V., Edie, S.M., Guo, W. (2023) Biologically driven isotopic fractionations in bivalves: from palaeoenvironmental problem to palaeophysiological proxy. *Biological Reviews* 98, 1016–1032. https://doi.org/10.1111/brv.12940

Davies, A.J., Guo, W., Bernecker, M., Tagliavento, M., Raddatz, J., Gischler, E., Floegel, S., Fiebig, J. (2022) Dual clumped isotope thermometry of coral carbonate. *Geochimica et Cosmochimica Acta* 338, 66–78. https://doi.org/10.1016/j.gca.2022.10.015

Davies, A.J., Brand, U., Tagliavento, M., Bitner, M.A., Bajnai, D., Staudigel, P., Bernecker, M., Fiebig, J. (2023) Isotopic disequilibrium in brachiopods disentangled with dual clumped isotope thermometry. *Geochimica et Cosmochimica Acta* 359, 135–147. https://doi.org/10.1016/j.gca.2023.08.005

Fiebig, J., Bajnai, D., Löffler, N., Methner, K., Krsnik, E., Mulch, A., Hofmann, S. (2019) Combined high-precision Δ_{48} and Δ_{47} analysis of carbonates. *Chemical Geology* 522, 186–191. https://doi.org/10.1016/j.chemgeo.2019.05.019

Fiebig, J., Daëron, M., Bernecker, M., Guo, W., Schneider, G., Boch, R., Bernasconi, S.M., Jautzy, J., Dietzel, M. (2021) Calibration of the dual clumped isotope thermometer for carbonates. *Geochimica et Cosmochimica Acta* 312, 235–256. https://doi.org/10.1016/j.gca.2021.07.012

Fiebig, J., Bernecker, M., Meijer, N., Methner, K., Staudigel, P.T., Davies, A.J., Bayarjargal, L., Spahr, D., Winkler, B., Hofmann, S., Granzin, M., Petersen, S.V. (2024) Carbonate clumped isotope values compromised by nitrate-derived NO_2 interferent. *Chemical Geology* 670, 122382. https://doi.org/10.1016/j.chemgeo.2024.122382

Gey, C.J., Pfister, L., Türk, G., Thielen, F., Leonard, L., Schmitt, K.E., Schöne, B.R. (2024) Biologically driven isotope fractionation in ultrastructurally different shell portions of freshwater pearl mussels (*Margaritifera margaritifera*): Implications for stream water $\delta^{18}O$ reconstructions. *Limnology and Oceanography Letters* 9, 827–836. https://doi.org/10.1002/lol2.10426

Ghosh, P., Adkins, J., Affek, H., Balta, B., Guo, W., Schauble, E.A., Schrag, D., Eiler, J.M. (2006) ^{13}C–^{18}O bonds in carbonate minerals: A new kind of paleothermometer. *Geochimica et Cosmochimica Acta* 70, 1439–1456. https://doi.org/10.1016/j.gca.2005.11.014

Gillikin, D.P., Lorrain, A., Meng, L., Dehairs, F. (2007) A large metabolic carbon contribution to the $\delta^{13}C$ record in marine aragonitic bivalve shells. *Geochimica et Cosmochimica Acta* 71, 2936–2946. https://doi.org/10.1016/j.gca.2007.04.003

Hill, P.S., Tripati, A.K., Schauble, E.A. (2014) Theoretical constraints on the effects of pH, salinity, and temperature on clumped isotope signatures of dissolved inorganic carbon species and precipitating carbonate minerals. *Geochimica et Cosmochimica Acta* 125, 610–652. https://doi.org/10.1016/j.gca.2013.06.018

Huntington, K.W., Petersen, S.V. (2023) Frontiers of Carbonate Clumped Isotope Thermometry. *Annual Review of Earth and Planetary Sciences* 51, 611–641. https://doi.org/10.1146/annurev-earth-031621-085949

Kelson, J.R., Huntington, K.W., Schauer, A.J., Saenger, C., Lechler, A.R. (2017) Toward a universal carbonate clumped isotope calibration: Diverse synthesis and preparatory methods suggest a single temperature relationship. *Geochimica et Cosmochimica Acta* 197, 104–131. https://doi.org/10.1016/j.gca.2016.10.010

Locarnini, R.A., Mishonov, A.V., Baranova, O.K., Reagan, J.R., Boyer, T.P., Seidov, D., Wang, Z., Garcia, H.E., Bouchard, C., Cross, S.L., Paver, C.R., Dukhovskoy, D. (2024) World Ocean Atlas 2023, Volume 1: Temperature. *NOAA Atlas NESDIS* 89. https://doi.org/10.25923/54bh-1613

Lollos, D.M., Curley, A.N., Petersen, S.V. (2025) Regional variation in biologically driven isotopic fractionations in cosmopolitan bivalve genera *Dosinia* and *Mactra*. *PALAIOS* 40, 321–335. https://doi.org/10.2110/palo.2025.004

Purba, M.M., Fajri, N.E., Yuliati, Y. (2025) Bioecology of lokan calm (*Geloina erosa*) in the mangrove ecosystem of Buruk Bakul village, Bukit Batu district, Bengkalis regency, Riau province. *Aurelia Journal* 7, 55–66. https://doi.org/10.15578/aj.v7i1.14329

Schauble, E.A., Ghosh, P., Eiler, J.M. (2006) Preferential formation of ^{13}C–^{18}O bonds in carbonate minerals, estimated using first-principles lattice dynamics. *Geochimica et Cosmochimica Acta* 70, 2510–2529. https://doi.org/10.1016/j.gca.2006.02.011

Schlidt, V., Evans, D., de Winter, N.J., Bernecker, M., Arndt, I., Staudigel, P.T., Davies, A.J., Brand, U., Müller, W., Fiebig, J. (2025) Most bivalves and gastropods calcify indistinguishably from dual clumped isotope equilibrium. *Geochimica et Cosmochimica Acta* 410, 174–187. https://doi.org/10.1016/j.gca.2025.10.008

Soeprobowati, T.R., Jumari, J., Wasiq Hidayat, J., Muhammad, F., Hanif Al Falah, M., Kadek Dita Cahyani, N., Gell, P. (2023) Water Quality Status of Mangrove Ecosystem in Bedono, Sayung, Demak, Central Java. *Pollution* 9, 1374–1385. https://doi.org/10.22059/poll.2023.355899.1803

Staudigel, P.T., Swart, P.K. (2016) Isotopic behavior during the aragonite-calcite transition: Implications for sample preparation and proxy interpretation. *Chemical Geology* 442, 130–138. https://doi.org/10.1016/j.chemgeo.2016.09.013

Staudigel, P., Davies, A.J., Bernecker, M., Tagliavento, M., van der Lubbe, H.J.L., Nooitgedacht, C., Looser, N., Bernasconi, S.M., Vonhof, H., Fiebig, J. (2023) Fingerprinting Kinetic Isotope Effects and Diagenetic Exchange Reactions Using Fluid Inclusion and Dual-Clumped Isotope Analysis. *Geochemistry, Geophysics, Geosystems* 24, e2022GC010766. https://doi.org/10.1029/2022GC010766

Staudigel, P., Bernecker, M., Curley, A., Meijer, N., Bayarjargal, L., Dietzel, M., Fiebig, J. (2025) Isotopic resetting of CO_2 in the presence of carbonate samples: Implications for oxygen- and clumped-isotope analyses. *Chemical Geology* 694, 123012. https://doi.org/10.1016/j.chemgeo.2025.123012

Vilibić, I., Dunić, N., Peharda, M. (2022) Near-surface ocean temperature variations across temporal scales in the coastal eastern Adriatic. *Continental Shelf Research* 245, 104786. https://doi.org/10.1016/j.csr.2022.104786